INTECH
open science | open minds

OPEN ACCESS
ARTICLE

International Journal of Advanced Robotic Systems

The Structure and Dimensional Design of a Reconfigurable PKM

Regular Paper

Xiaoqiang Tang[1,*], Dengfeng Sun[2] and Zhufeng Shao[1]

1 The State Key Laboratory of Tribology, Department of Precision Instruments and Mechanology, Tsinghua University,Beijing, P.R. of China
2 School of Aeronautics and Astronautics Engineering, Purdue University, West Lafayette, IN,USA
* Corresponding author E-mail:tang-xq@mail.tsinghua.edu.cn

Received 4Oct 2012; Accepted 26Oct 2012

DOI: 10.5772/54696

Abstract Parallel Kinematic Machines (PKMs) have many advantages and have been widely used in the machine industry. Benefitting from its modular structure, a PKM is more reconfigurable than traditional serial machines. In this paper, a new type of driving strut module and innovative joints are designed for the Reconfigurable Parallel Kinematic Machine (RPKM). The new driving strut module can be changed from linear drive mode to telescopic drive mode easily, and the new spherical joint and universal joint are designed to achieve a large rotation angle. The inverse kinematics problems in relation to the 6-DOF RPKM are analysed, and the Workspace Volume Index (WVI) and the Global ConditionIndex (GCI) are adopted to design the RPKM. According to the WVI and GCI analysis of the selected parameters for two types of 6-DOF PKM, the dimensional parameters of the RPKM are designed. In the end, the new type of RPKM prototype is built, with which a wax pattern is machined.

Keywords Structure Design, Dimensional Design, Reconfigurable PKM

1. Introduction

In recent years, the ever-changing manufacturing environment caused by intensive competition on a global scale and rapid changes in process technology has led to the requirement for an increasingly efficient production system. In order to achieve this, a reconfigurable manufacturing system characterized by modularity, integrability, customization, convertibility and diagnosability, which can easily be reconfigured and respond to unpredictable market changes cost-effectively, is highly preferred. The earliest large-scale research on reconfigurable manufacture systems reported in the literature is the Flexible Manufacture Cell (FMC) project launched in 1977 by MITI in Japan. Other reconfiguration projects, such as MOSYN, KERNEL and MOTION, focused on modular machine tools. After the foundation of the Engineering Research Center of Reconfigurable Machining Systems (ERC/RMS) at the University of Michigan in 1996, researchers began to develop the theory and technology of reconfigurable manufacturing systems systematically[1-3].

A Parallel Kinematic Machine (PKM) has many advantages and has been widely used in machine industry. Thanks to its modular structure, a PKM is more reconfigurable than the traditional serial machine. With the modular design, several modules of PKMs can be integrated into a module set so that the modules can be reassembled rapidly for different applications. As a result, the recent trend in reconfigurable manufacturing

systems has promoted the research and development of a novel type of machine tool called a Reconfigurable Parallel Kinematic Machine (RPKM) [4-5], which is based on the parallel manipulator.

More recently, the research on RPKMs has made some substantive progress, but some problems that should be solved for its further application still exist [6-7]. Firstly, according to drive mode, the PKM can be mainly classified into two kinds: the telescopic drive PKM, whose struts are extendable with one end mounted on framework or base platform and the other on the moving platform; the linear drive PKM, whose struts have constant length with one end mounted on a slider and the other on the moving platform. Because both these PKMs have their pros and cons, they are designed and applied in respective cases: the linear drive PKM is inclined to be adopted in machining long-shaped parts along its dominant movement direction, and the telescopic drive PKM is suitable to machine more complicated shapes other than those of a longshape [8]. It would therefore be ideal if the RPKM can realize these two types of PKMs with the same modular set. Moreover, these two types of PKMs need to use the universal joints and spherical joints. A universal joint can work with 2-DOFs rotation, and a spherical joint with 3-DOFs rotation. With the classic manufacturing process, it is difficult to fabricate a high precision spherical joint with a large rotation angle. To solve this problem, an integrated joint with either two DOFs or three DOFs should be designed.

The dimensional design is another important and challenging problem for RPKMs. Two major issues need to be addressed in the optimal design of a PKM: performance evaluation and synthesis. After the design of a RPKM, it is necessary to evaluate its main characteristics. The second problem is to determine the dimensions (link lengths) of the RPKM, to make it most suitable for the specific task. The latter problem is one of the most difficult issues to solve in the field of RPKM. As is well known, the performances of parallel kinematic machines mainly depend upon the dimensions. Therefore, the process of mechanism dimensional design for a manipulator is largely based on the usage of the criteria, such as workspace, dexterity, payload, conditioning index and stiffness [9-11]. Approaches in previous work dealing with the dimensional design of PKMs can be classified into two categories. One category refers to the local optimal design [11-13], focusing on finding a family of dimensional parameters that generate an isotropy configuration, where the platform presents the desirable characteristics in terms of kinematics accuracy, noise rejection and singularity avoidance. However, due to the possible strut interference, this family of design parameters would not be useful in the design where the desirable orientation capability of the moving platform is also required. The other category refers to the global optimal design [14,15], which attempts to find a set of design parameters to minimize a weighted cost function in terms of the specified dexterous performance and workspace volume. The reason for implementing global optimal design would be that kinematics performance could not be guaranteed simply by conducting local optimal design. However, the above two dimensional design methods are only used for the telescopic drive PKM or the linear drive PKM respectively. In this paper, we will try to use the global optimal design method to designthe RPKM.

In this paper, a new type of driving struts moduleand joints are designed for the RPKM. The inverse kinematics problems with regard to the two types of 6-DOF parallel manipulators are described and a global optimal design index is used to design the RPKM, which can satisfy the requirement of the RPKM and realize workspace and dexterity capability. In the end, we show two wax patterns milled by the RPKM.

2. Structure design

The structure of reconfigurable PKMs is similar to that of some ordinary PKMs. They consist of common parts like: a base platform, a moving platform on which ending executor is installed, and some parallel-actuated extendible legs or movable legs between the mobile and base platforms. Universal joints and spherical joints are mounted on either the moving platform or the base platform to connect platforms and legs, and to provide multi-position and versatile attitude.

The key modular designs of reconfigurable PKMs include strut modules and joint modules.

2.1 Strut modules design [16]

According to driving mode, PKMs can mainly be catalogued into two kinds: telescopic drive PKMs, whose struts are extendable with one end mounted on the framework or base platform and the other on the moving platform; linear drive PKMs, whose struts have constant length with one end mounted on a slider and the other on the moving platform.

In figure 1, the telescopic drive mode is represented: a driving motor (1) is mounted at one end of the telescopic drive module. The motor drives the ball screw (2), and the work-piece module (3) moves along the axis of the ball screw (2). A rod-fix module (4) is connected to the work-piece module along the direction of the screw in the linear drive module, then a constant-length rod module (5) and a spherical joint (6) are mounted in turn. The length of the rod module (5) is represented by l_k , and the maximal move distance of the telescopic drive mode is denoted by Δl .

In figure 2, linear drive mode is represented as follows: a driving motor(1) is mounted at one end of the linear drive module, the motor drives the ball screw(2), and the work-piece module(3) moves along the axis of the ball screw(2). A universal joint (7) is mounted on the work-piece module, then a rod-fix module (4) is connected to the constant-length rod module (5) and a spherical joint (6) are mounted in turn. The length of rod module (5) is represented by l_k, and the maximal move distance is represented by Δl.

According to the design, the telescopic drive mode can be changed into linear drive mode by mounting the constant-length rod module (5)at another place on the work-piece module (3). The assembling process is very easy and can be finished in a short period of time.

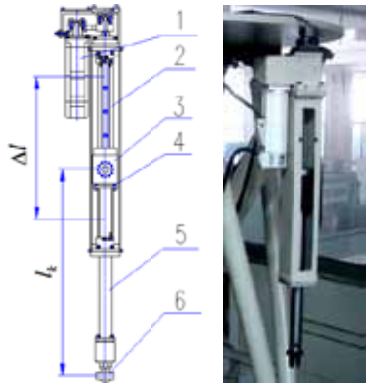

Figure 1. Telescopic drive mode

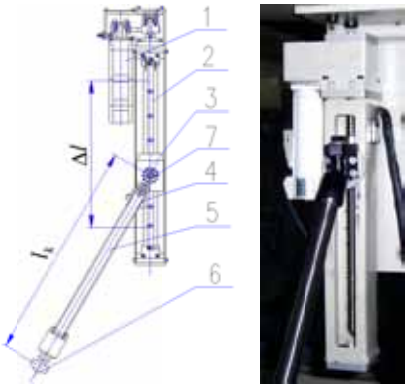

Figure 2. Linear drive mode.

2.2 Joint module design [17]

In a RPKM, a universal joint has two DOFs, and a spherical joint has three DOFs. With the classic manufacturing process, it is difficult to fabricate a high precision spherical joint. Moreover, the general rotation angle of the traditional spherical joint is no more than $\pm 20^{\circ}$. To resolve this issue, integrated joints possessing either two DOFs or three DOFs are designed, as shown in figure 3. The new type of spherical joint includes three rotation axes, which are C- axis, A-axis and C-axis with three DOFs. As shown in figure 4, whenwe use two rotation axes only, the spherical joint will be changed into universal joint with two DOFs.

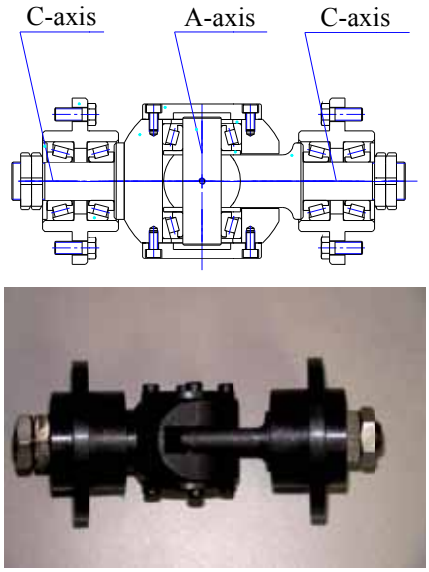

Figure 3. Spherical joint

The rotation angle of C-axis is $\pm 90^{\circ}$ and the rotation angle of A-axis is $\pm 60^{\circ}$, so the general rotation angle of the new type spherical joint and universal joint is $\pm 60^{\circ}$.

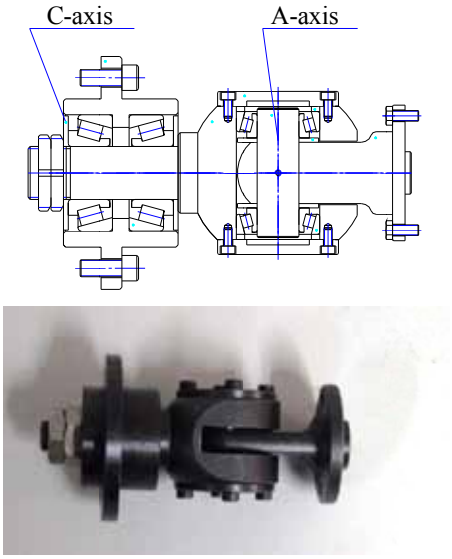

Figure 4. Universal joint

2.3 Two types of 6-DOF PKMs

Both the linear drive PKM and the telescopic drive PKM have their pros and cons. Therefore, they are generally designed to be applied in respective cases: the linear drive PKM is inclined to be adopted in machining long-shaped parts along its linear movement direction, and the telescopic drive PKM is suitable to machine more complicated shapes other than those of a longshape. As shown in figures 5 and 6, we assemble two types of PKMs with the same module set.

Figure 5. The telescopic drive PKM

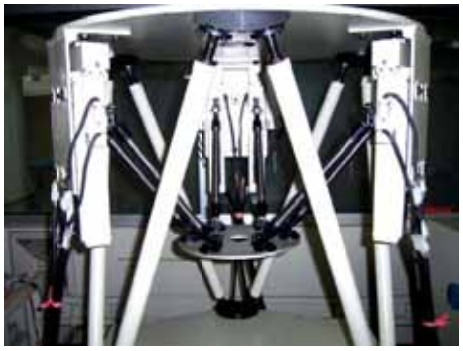

Figure 6. The linear drive PKM

3. Dimensional design

As soon as we have the structure design of the RPKM, the most important step is to decide the dimensions of the RPKM. It is of primary importance to develop a useful design method that can reveal the relationships between the criteria and link dimensions of the machine. Firstly, the kinematics model of the RPKM is built and the criteria indexes are formulated. Then we get the dimensional results through analysing the Workspace Volume Index (*WVI*) and the Global Conditioning Index (*GCI*) [14].

3.1 Kinematics model

Kinematics models of these two types of PKM are developed as shown in figure 7. The vertices of the moving platform are denoted as platform joints A_i $(i=1,2,3,...,6)$, and the vertices of the base plate are denoted as B_i $(i=1,2,3,...,6)$. A fixed global reference system $\Re: o-xyz$ is located at the centre of the circle $B_1...B_6$ with the z axis vertical to the base plate and the y axis in coincidence with OB_1. The circumcircle radius of points $B_1...B_6$ is denoted as R_B. Another reference frame, defining the top frame $\Re': o'-x'y'z'$, is located at the centre of the circle $A_1...A_6$. The z' axis is perpendicular to the moving platform and y' axis parallel to the vector $O'A_1$. The circumcircle radius of points $A_1...A_6$ is denoted as R_A. Vector A_iB_i is denoted as $\mathbf{L}_i$ $(i=1,2,3,...,6)$, and the link length for each leg is denoted as l, where $A_iB_i=l$, $(i=1,2,...,6)$. Because the structure is symmetrical, $\theta_B=2\pi/3-\phi_B$ and $\theta_A=2\pi/3-\varphi_A$.

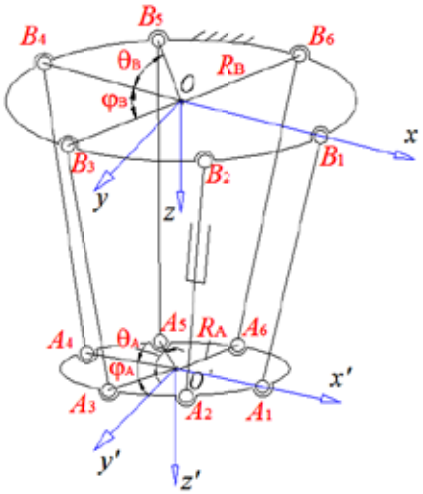

a. The telescopic drive PKM

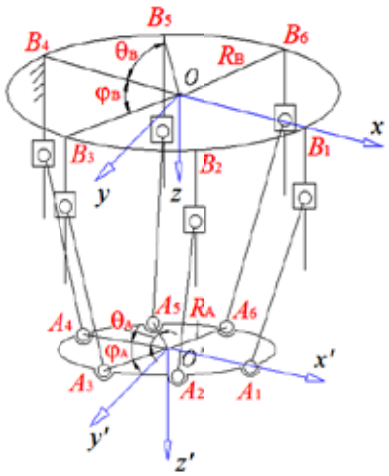

b. The linear drive PKM

Figure 7. The geometric architecture of the 6-DOF parallel manipulators.

The objective of the inverse kinematics solution is to define a mapping from the pose of the moving platform in the Cartesian space to the set of actuated leg inputs in order to achieve the aim pose. For this analysis, the pose of the moving platform is assumed to be known. The position is given by the position vector $\left[O'\right]_{\Re}$ and the orientation is given by a matrix $\mathbf{R}$. Then it is shown

$$\left[\boldsymbol{O}'\right]_{\Re}=\begin{pmatrix}x & y & z\end{pmatrix}^{T} \tag{1}$$

The rotation of coordinate system $\Re'$ relative to $\Re$ can be expressed by the rotation matrix

$$\mathbf{R}=\begin{bmatrix} c\gamma c\beta & c\gamma s\beta s\alpha-s\gamma c\alpha & c\gamma s\beta c\alpha+s\gamma s\alpha \\ s\gamma c\beta & s\gamma s\beta s\alpha+c\gamma c\alpha & s\gamma s\beta c\alpha-c\gamma s\alpha \\ -s\beta & c\beta s\alpha & c\beta c\alpha \end{bmatrix} \tag{2}$$

The vectors $\left[\boldsymbol{B}_i\right]$ in the base platform coordinate system $\Re$ can be written as:

$$\left[\mathbf{B}_i\right]_{\Re}=\left[R_B\cos((i-1)\cdot\pi/3),R_B\sin((i-1)\cdot\pi/3),z_i\right],(i=1,3,5)$$

$$\left[\mathbf{B}_i\right]_{\Re}=\begin{bmatrix}R_B\cos((i-2)\cdot\pi/3+\phi_B),\\ R_B\sin((i-2)\cdot\pi/3+\phi_B),z_i\end{bmatrix}\quad(i=2,4,6)\tag{3}$$

where $z_i=0,i=1...6$, for PKM with telescopic drives.

The vectors $\left[\boldsymbol{A}_i\right]$ in the moving platform coordinate system $\Re'$ can be written as:

$$\left[\mathbf{A}_i\right]_{\Re'}=\left[R_A\cos((i-1)\cdot\pi/3),R_A\sin((i-1)\cdot\pi/3),0\right],(i=1,3,5)$$

$$\left[\mathbf{A}_i\right]_{\Re'}=\begin{bmatrix}R_A\cos((i-2)\cdot\pi/3+\phi_A),\\ R_A\sin((i-2)\cdot\pi/3+\phi_A),0\end{bmatrix},\quad(i=2,4,6)\tag{4}$$

Therefore, the vectors $\left[\boldsymbol{A}_i\right]$ can be expressed in the base platform coordinate system $\Re$ as:

$$\left[\boldsymbol{A}_i\right]_{\Re}=\mathbf{R}\left[\boldsymbol{A}_i\right]_{\Re'}+\left[\boldsymbol{O}'\right]_{\Re},\qquad(i=1,2,...,6)\tag{5}$$

The relationship between vectors $\left[\boldsymbol{A}_i\right],\left[\mathrm{B}_i\right]$ and strut vectors has the following form according to the geometric constraint of the architecture:

$$\left\|\left[\boldsymbol{B}_i\right]_{\Re}-\left[\boldsymbol{A}_i\right]_{\Re}\right\|=\left\|\boldsymbol{L}_i\right\|=l_i,\quad(i=1,2,...,6)\tag{6}$$

where $l_i=l_k,i=1,2,...,6$ if the PKM is equipped with linear drives.

The inverse kinematics problem of the machine can be solved by Eq. (6), where the unknown items are either l_i ($i=1,2,...,6$) for the PKM with telescopic drives, or z_i ($i=1,2,...,6$) for the PKM with linear drives.

Hence, for a given mechanism and prescribed position and orientation of the moving platform, the required actuator inputs can be directly computed from Eq. (6).

Eq. (6) can be differentiated with respect to time to obtain the velocity equation. This leads to an equation as:

$$\mathbf{J}_p\dot{\boldsymbol{p}}=\mathbf{J}_q\dot{\boldsymbol{q}}\tag{9}$$

where $\dot{\boldsymbol{q}}$ is the velocity vector of the moving platform defined in the Cartesian coordinate systemas

$$\dot{\boldsymbol{q}}=\left[\dot{x},\dot{y},\dot{z},\dot{\alpha},\dot{\beta},\dot{\gamma}\right]^{\mathrm{T}}\tag{10}$$

and $\dot{\boldsymbol{p}}$ is the vector of input velocities. As mentioned earlier, there are two different types of drive modes. When the PKM is equipped with telescoped legs, $\dot{\boldsymbol{p}}$ can be expressed as

$$\dot{\boldsymbol{p}}=[\dot{l}_1,\dot{l}_2,\dot{l}_3,\dot{l}_4,\dot{l}_5,\dot{l}_6]^{\mathrm{T}}\tag{11}$$

while when the PKM is actuated with slider legs, its expression is

$$\dot{\boldsymbol{p}}=[\dot{z}_1,\dot{z}_2,\dot{z}_3,\dot{z}_4,\dot{z}_5,\dot{z}_6]^{\mathrm{T}}\tag{12}$$

Matrices $\mathbf{J}_p$ and $\mathbf{J}_q$ are the 6×6 forward and inverse Jacobian matrices of the mechanism, and can be expressed as

$$\mathbf{J}_p=\begin{bmatrix}J_{p1}&&&&&\\&J_{p2}&&&0&\\&&J_{p3}&&&\\&&&J_{p4}&&\\&0&&&J_{p5}&\\&&&&&J_{p6}\end{bmatrix}_{6\times6}\tag{13}$$

$$\mathbf{J}_q=\begin{bmatrix}\mathbf{w}_1&(\mathbf{v}_1\times\mathbf{w}_1)\\ \mathbf{w}_2&(\mathbf{v}_2\times\mathbf{w}_2)\\ \mathbf{w}_3&(\mathbf{v}_3\times\mathbf{w}_3)\\ \mathbf{w}_4&(\mathbf{v}_4\times\mathbf{w}_4)\\ \mathbf{w}_5&(\mathbf{v}_5\times\mathbf{w}_5)\\ \mathbf{w}_6&(\mathbf{v}_6\times\mathbf{w}_6)\end{bmatrix}_{6\times6}\tag{14}$$

where $\mathbf{w}_i$ is the unit vector of $\boldsymbol{L}_i$ and $\mathbf{v}_i=\mathbf{R}_1\left[\mathbf{A}_i\right]_{\Re'}$. $\mathbf{J}_q=\mathbf{I}$, $\mathbf{J}_{qi}=1,(i=1,2,...,6)$;

When the PKM is actuated with telescoped legs, $\mathbf{J}_{qi}=1,(i=1,2,...,6)$ and $\mathbf{J}_q=\mathbf{I}$; if the PKM is equipped with slider legs, $\mathbf{J}_{qi}=(\mathbf{w}_i)_z$, where $(\mathbf{w}_i)_z$ is the third element of vector $\mathbf{w}_i$ with respect to the z axis coordinate. If the $\left\|\mathbf{J}_q\right\|\neq0$, the equation can be written as:

$$\dot{\mathbf{p}}=\mathbf{J}_p^{-1}\mathbf{J}_q\dot{\mathbf{q}}=\mathbf{J}\dot{\mathbf{q}}\tag{15}$$

3.2 Workspace and index

The workspace of a PKM is the work region which the tool can reach, and is an important indication of the PKM's performance. In this section, the Workspace Volume Index (***WVI***) is used to represent the workspace volume of the RPKM. A numeric method is applied to compute the PKM's reachable points to integrate the workspace surface. According to the earlier research of Huang [13], the same optimal design result for workspace can be obtained by setting the rotation angles of the moving platform to zero or other values. To simplify the analysis, the three rotation angles of the moving platform are all set to zero in this calculation.

If we are given the initial value as shown in Table 1, the workspaces of the two kinds of PKMs are shown in figure 8 and their WVIs are $1.5\text{x}10^8$ mm^3 and $1.2\text{x}10^7$ mm^3 respectively.

Dimensional Variable	Description	Initial Value
R_A (mm)	Radius of base platform	200
R_B (mm)	Radius of moving platform	400
Δl (mm)	The maximal move range of strut	200
θ_A (°)	The strut mounted angle on moving platform(figure 7)	60(π / 3)
θ_B (°)	The strut mounted angle on base platform(figure 7)	30(π / 6)
PKM with telescopic legs		
l_{min} (mm)	Minimal length of telescopic legs	500
$l_{max} = l_{min} + \Delta l$ (mm)	Maximal length of telescopic legs	700
PKM with linear legs		
z_{min} (mm)	Maximal height of work-piece module	200
$z_{max} = z_{min} + \Delta l$ (mm)	Minimal height of work-piece module	400
l_k (mm)	Length of rod module	600

Table 1. The dimensional variables

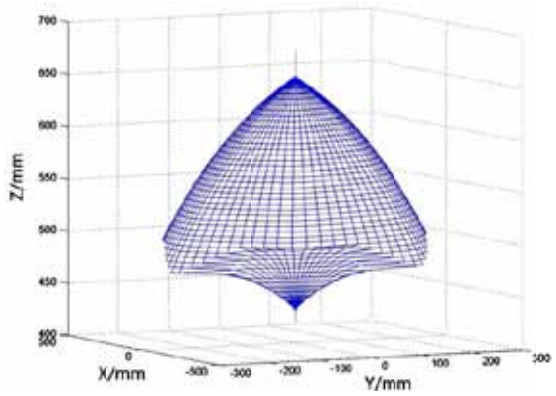

a. The telescopic drive PKM

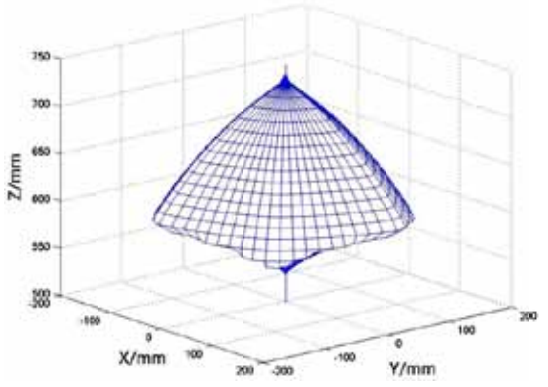

b. The linear drive PKM

Figure 8. RPKM workspace surface

3.3 Conditional number and GCI index

The condition number of Jacobian matrix **J** can be used to evaluate the dexterity [18]. The condition number expression is written as:

$$k_1 = \delta_1 / \delta_6 \tag{16}$$

where δ_i (i=1,2,…,6) are the singularity values of the Jacobian matrix **J** .

According to the characteristic equation of singularity value

$$\det(\lambda' \mathbf{E}_6 - \mathbf{J}^T \mathbf{J}) = 0 \tag{17}$$

The singularity value is

$$\delta_i = \sqrt{\lambda_i'(\mathbf{J}^T \mathbf{J})}\ , \text{(i=1…6)} \tag{18}$$

Now, the Local Conditioning Index (*LCI*) is used to evaluating the performance of the RPKM, which is:

$$LCI = 1 / k_1 = \delta_6 / \delta_1 \tag{19}$$

It has been acknowledged that a larger value of *LCI* indicates a better motion dexterity of the moving platform. As shown in figure 9, given the dimensional variables in Table1, the change trends of the *LCI* value can be shownin one X-Y plane of the workspace.

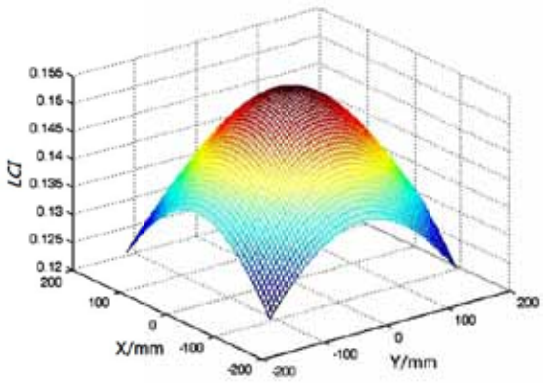

a. The telescopic drive PKM

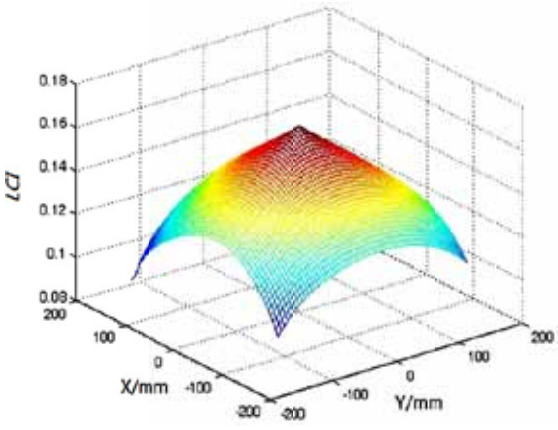

b. The linear drive PKM

Figure 9.*LCI* of RPKM

However, the *LCI* can only evaluate the dexterity of X-Y plane forthe PKM workspace, and we adopt Global

Condition Index (*GCI*) [14] to evaluate the dexterity of whole workspace, a promising approach defined as

$$\mathrm{GCI} = \int_W 1/\mathrm{k}_1 \mathrm{dW} \Big/ \int_W \mathrm{dW} \tag{20}$$

where dW is a differential workspace volume, and k_1 is the condition number of the Jacobian matrix at a given moving platform pose, which is defined as the ratio of maximum and minimum singularity values of the manipulator Jacobian matrix. It is well known that a larger value of *GCI* reveals a better motion dexterity of the moving platform.

3.4 Workspace and GCI analysis

From Table 1, we can know that ten dimensional variables should be designed. It will be very difficult to analyse all the variables at one time. So the discussed design variables are defined as $\mu_1 = \theta_A$, $\mu_2 = \theta_B$, $\mu_3 = \mathrm{R_A}/\Delta\mathrm{l}$, $\mu_4 = \mathrm{R_B}/\Delta\mathrm{l}$, $\mu_5 = \mathrm{l_{min}}/\Delta\mathrm{l}$ and $\mu_6 = \mathrm{l_k}/\Delta\mathrm{l}$, where μ_3, μ_4, μ_5 and μ_6 are all dimensionless variables. Based on the workspace and formula of *GCI*, the effects of the design variables on the dexterity and workspace can be discussed and evaluated. The ball screw length limitation gives $\Delta\mathrm{l} = 200\mathrm{mm}$. Other design parameters that are not discussed below are the same as specified in Table 1.

3.4.1 Workspace effect analysis

Figure 10 shows the *WVI* curve when μ_1 and μ_2 are given different values. It indicates that the workspace expands as μ_1 increases. When $\mu_2 = 30^\circ$, the maximal workspace volume can be obtained. Because the proposed RPKM structures are symmetrical, the value of μ_1 should not be larger than 60°, so we will let $\mu_1 = 60^\circ$ and $\mu_2 = 30^\circ$ for the following analysis.

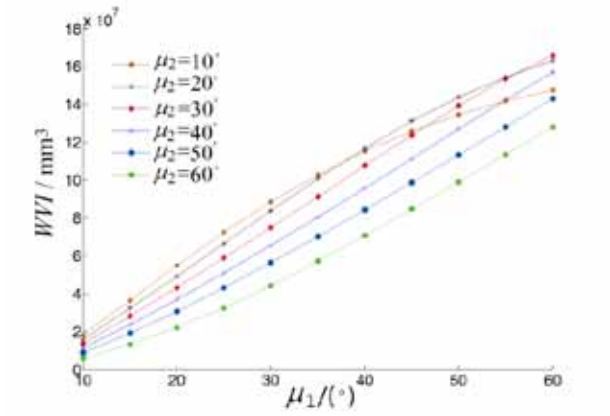

a. The telescopic drive PKM

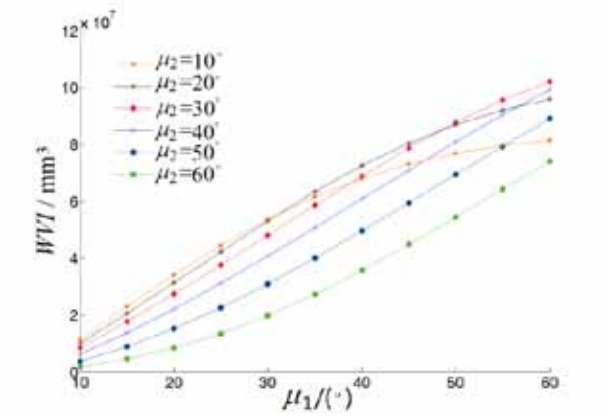

b. The linear drive PKM

Figure 10. Workspace volumes of RPKM with different μ_1 & μ_2

As shown in figure 11, the workspace volumes increase with μ_3 increasing and μ_4 decreasing. If we only want to get the largest workspace volume, selecting the largest value of μ_3 and the smallest value of μ_4 will be a good choice.

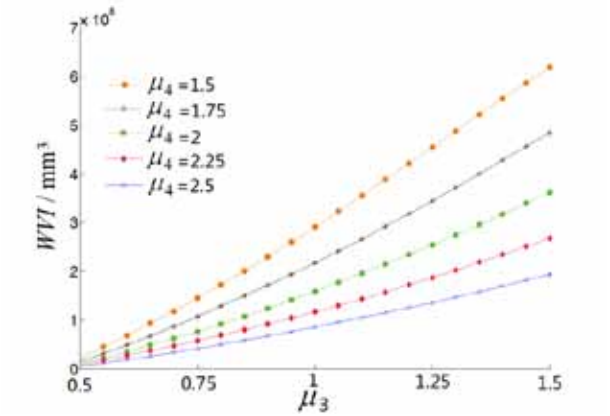

a. The telescopic drive PKM

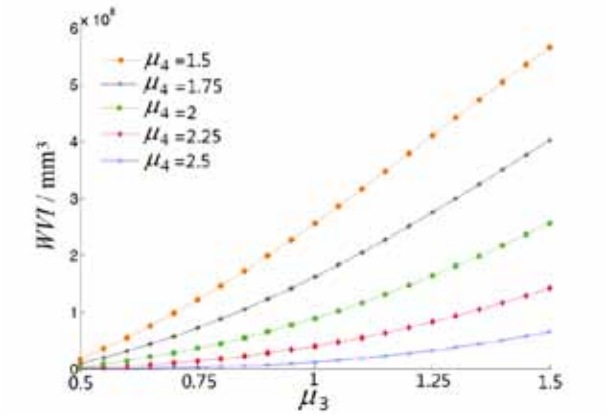

b. The linear drive PKM

Figure 11. Workspace volumes of the RPKM with different μ_3 and μ_4

As shown in figure 12, the design variable μ_5 only has impact on the workspace volumes of the telescopic drive PKM, while the design variable μ_6 only affects the workspace volumes of the linear drive PKM. Workspace increases with μ_5 increasing and μ_4 decreasing. Workspace volumes increase as μ_6 increases and μ_4 decreases. If we only want to get the largest workspace, selecting the largest values of μ_5 and μ_6 will be a good choice. However, the increasing values of μ_5 and μ_6 will decrease the stiffness of the machine.

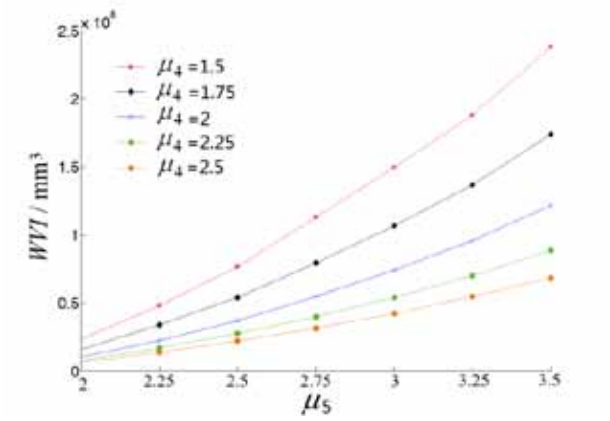

a. The telescopic drive PKM

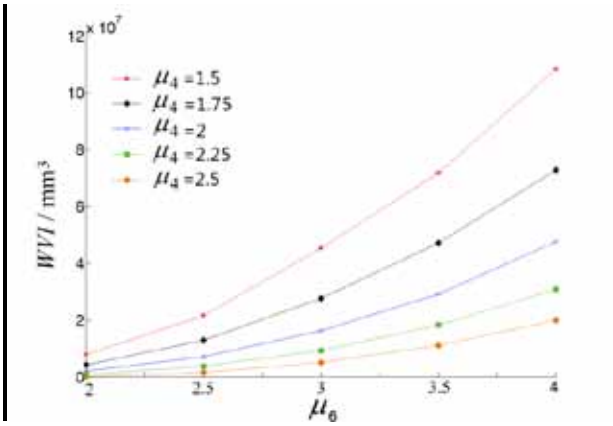

b. The linear drive PKM

Figure12. Workspace volumes of the RPKM with different μ_4 , μ_5 and μ_6

3.4.2 GCI effect analysis

As shown in figure 13, we can get the maximal *GCI* as long as the value of μ_3 is close to one, and the values of *GCI* increase as μ_4 decreases.

As shown in figure 14, the design variable of μ_5 only affects the *GCI* of the telescopic drive PKM, while the design variable of μ_6 only affects the linear drive PKM. The maximal value of *GCI* can be obtained as the value of μ_5 and μ_6 are near 2.5. The values of *GCI* increase when μ_4 increases.

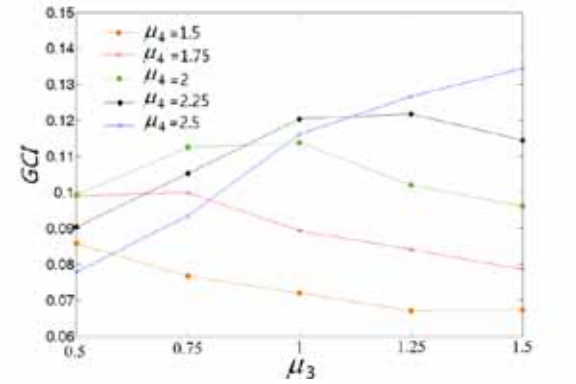

a. The telescopic drive PKM

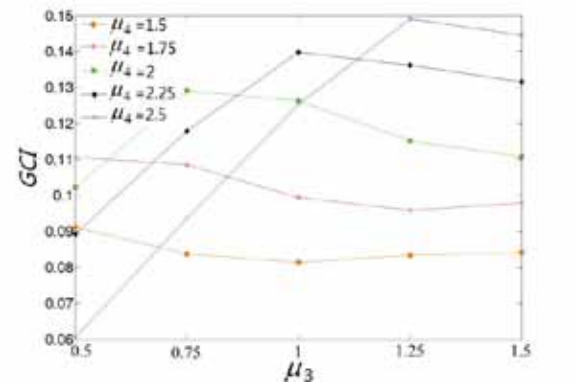

b. The linear drive PKM

Figure 13.*GCI* of the RPKM with different μ_3 and μ_4

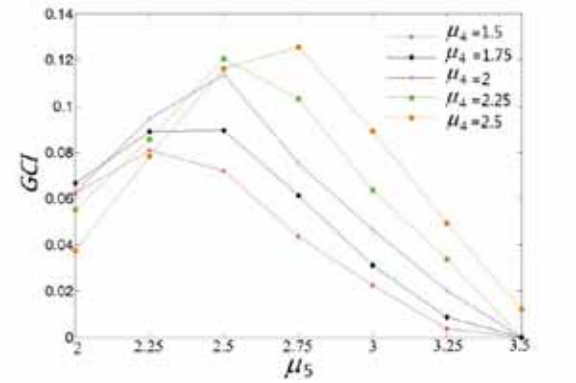

a. The telescopic drive PKM

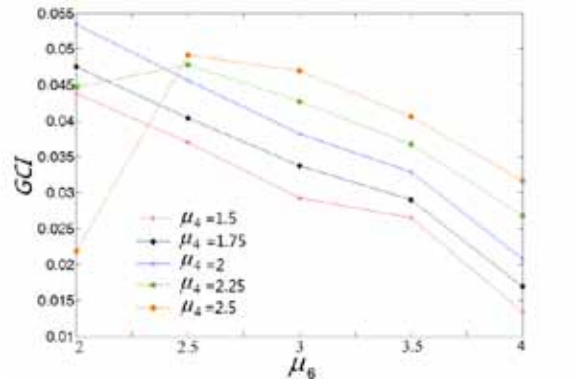

b. The linear drive PKM

Figure14.*GCI* of the RPKM with different μ_4 , μ_5 and μ_6

3.5 Dimensional variables design

The dimensional variables effects on *WVI* and *GCI*are shown in Table 2.

Dimensional variables	μ_1	μ_2	μ_3
Getting larger WVI	60°	30°	The largest value
Getting larger GC	--	--	Near 1
Dimensional variables	μ_4	μ_5	μ_6
Getting larger WVI	The smallest value	The largest value	The largest value
Getting larger GC	The largest value	Near 2.5	Near 2.5

Table 2. The dimensional variables effects on *WVI* and *GCI*

According to the definition of WVI and *GCI*, larger values of *WVI* and *GCI* indicate a larger workspace volume and a better motion dexterity of moving platform. If we only analyse the workspace, design variables should be selected as $\mu_1 = 60^\circ$, $\mu_2 = 30^\circ$, $\mu_3 = 1.5$, $\mu_4 = 1.5$, $\mu_5 = 3.5$ and $\mu_6 = 4$. However, the *GCI* is very important in the PKM's performance, so we should consider the GCI first, and then endeavour to obtain a larger workspace. Therefore, according to the GCI effect analysis results, the design variables are selected as $\mu_3 = 1$, $\mu_4 = 2.5$, $\mu_5 = 2.5$ and $\mu_6 = 2.5$. According to figures 11, 12, 13 and 14, when $\mu_3 = 1.25$, $\mu_4 = 2$, $\mu_5 = 3$ and $\mu_6 = 3$, the RPKM will get a larger workspace and reasonable GCI relatively. Then the dimensional variables can be calculated by the ratio of design parameters $\mu_i, i = 1,2,...,6$. Finally, the dimensional variables of the RPKM can be obtained and shown in Table 3.

Dimensional variables	R_A	R_B	Δl	θ_A (°)	θ_B (°)	l_{min}
Value	250	400	200	60	30	600
Dimensional variables	l_{max}	z_{min}	z_{max}	l_k	φ_A (°)	φ_B (°
Value	800	200	400	600	60	90

Table 3. The dimensional parameter of the RPKM prototype

Based on Table 3, a 6-DOF RPKM prototype was manufactured in 2010, as shown infigure 15.In figure 16(a), the telescopic drive PKM was machining one wax pattern, and in figure 16(b), the linear drive PKM prototype was machining another wax pattern, which proved the feasibility of the 6-DOF RPKM prototype.

4. Conclusion

In this paper, a 6-DOF RPKM is proposed, which can be assembled into either the telescopic drive PKM or the linear drive PKM with the same module set. Conclusions can be drawn as follows:

(1) A new type of strut is designed to realize either telescopic drive or linear drive without any other modules, where the telescopic drive mode can be changed into linear drive mode easily and in a short period of time.

(2) A compound joint with three rotation freedoms is designed to be a spherical joint, based on which a universal joint can also be obtained when one rotation is locked. Compared with traditional joints, the general rotation angle of the new type of spherical joint or universal joint is three times larger and can reach $\pm 60^\circ$.

(3) The indices of *WVI* and *GCI* are used to evaluate and design the variables of the 6-DOF RPKM. According to *WVI* and *GCI* analysis, the dimensionless variables are obtained, and then the prototype is built. Milling experiments proved that the new type of RPKM can implement the machining function.

However, only two 6-DOF PKMs are discussed in this paper. In the future work, we will design and research other RPKMswith the same drive mode and evaluation index.

a. The telescopic drive PKM

b. The linear drive PKM

Figure 15. The 6-DOF RPKM prototype

Milling by telescopic drive PKM

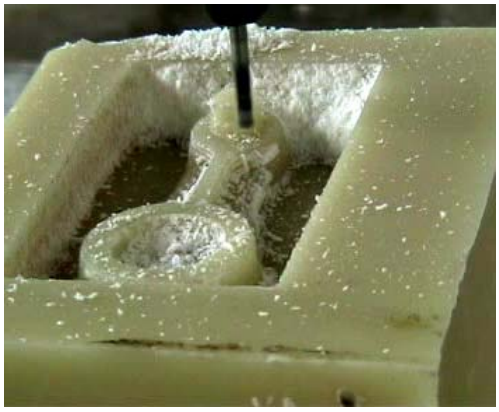

Milling by linear drive PKM

Figure 16. Milling wax pattern

5. Acknowledgments

This research is sponsored by the National Natural Science Foundation of China (nos. 11178012, 50975149), and the National S&T Major Project of China (no. 2011ZX04015-011).

6. References

[1] Y. Koren, A. G. Ulsoy, Reconfigurable Manufacturing Systems, Engineering Research Center for Reconfigurable Machining Systems(ERC/RMS), Report #1, The University of Michigan, Ann Arbor, MI, 1997.

[2] Y. Koren, Computer Control of Manufacturing Systems, McGraw-Hill, New York, 1983.

[3] Farhad, P. Kourosh, A Reconfigurable Robot With Lockable Cylindrical Joints, *IEEE Transactions on Robotics*, vol. 25,2009, pp. 785-797..

[4] F. Jovane, S. P. Negri, I. Fassi, L. Molinari Tosatti, Design Issues for Reconfigurable PKMs, in *2002 Parallel Kinematics Machines International Conference*, Germany, 2002, pp. 69-82..

[5] V. Angelo, L. Giovanni, et al., Performance analysis of a reconfigurable redundant parallel manipulator, in *The 2009 ASME/IFToMM International Conference on Reconfigurable Mechanisms and Robots*, King's College London, London, UK, 2009, pp. 647-655.

[6] X. Tang, C. Lin, et al., Structure Design and Task Planning of Reconfigurable Parallel Kinematic Machines System, in *The 2009 ASME/IFToMM International Conference on Reconfigurable Mechanisms and Robots*, King's College London, London, UK, 2009, pp. 175-182.

[7] G. Patrick, D. G. Raffaele, Planning for a Novel Reconfigurable Parallel Manipulator with Lockable Revolute Joints, in *2010 IEEE International Conference on Robotics and Automation*, Anchorage, Alaska, USA, 2010, pp. 4697-4702.

[8] X. Tang, J. Wang, M. Gao, Kinematic calibration of gantry hybrid machine tool based on estimation error and local measurement information, *International Journal of Advanced Manufacturing Technology*, vol. 26, 2005, pp. 382-390.

[9] K. H. Hunt, Structural kinematics of in-parallel-actuated robot arm, *ASME Transaction, AutomationDesign*, Vol. 4, 1983, pp. 705–712.

[10] Fattah and G. Kasaei, Kinematics and dynamics of a parallel manipulator with a new architecture, *Robotic*a, Vol. 18, 2000, pp. 535-543..

[11] X. Tang, R. Yao, Dimensional design on the six-cable driven parallel manipulator of FAST, *Journal of Mechanical Design*,vol. 133, 2011, pp. 1-12.

[12] K. H. Pittens, R.P. Podhordedski, A family of Stewart platforms with optimal dexterity. *Journal of Robotic Systems*, vol. 10, 1993, pp. 463-479.

[13] T. Huang, D. J. Whitehouse, J. Wang, Local dexterity, optimum architecture and design criteria of parallel machine tools. *CRIP Annals*, vol. 47,1998, pp. 347-351.

[14] C. Grosselin, J. Angels, A global performance index for the kinematic optimization of robotic manipulators. *Journal of Mechanical Design*, vol. 113, 1991, pp. 220-226.

[15] C. Grosselin, M. Guillot, The synthesis of manipulator with prescribed workspace, *Journal of Mechanical Design*, vol 113, 1991, pp. 451-455.

[16] J. Wang, X. Tang, C. Lin, G. Duan, J. Shi, Modular drive strut architecture for reconfigurable parallel kinematics machine. *Chinese Patents*, No. 03137758.0, 2003.

[17] X. Tang, J.S. Wang, C. S. Lin, et al., "An integrated joint for reconfigurable parallel kinematics machine", *Chinese Patents*, No. 200410000008.4, 2006.

[18] J. P. Merlet, Singular configurations of parallel manipulators and Grassmann geometry, in *Geometry and Robotics (Lecture Notes in Computer Science)*, New York: Springer-Verlag, vol. 391, 1989, pp. 194-212.